

Supporting Information

Integrated and heterostructured cobalt manganese sulfide nanoneedle arrays as advanced electrodes for high-performance supercapacitors

*Hui Peng^{‡a}, Gangang Wei^{‡a}, Kanjun Sun^b, Guofu Ma^{*a}, Enke Feng^a, Xue Yang^a, Ziqiang Lei^{*a}*

^aKey Laboratory of Eco-Environment-Related Polymer Materials of Ministry of Education, Key Laboratory of Polymer Materials of Gansu Province, College of Chemistry and Chemical Engineering, Northwest Normal University, Lanzhou 730070, China.

^bCollege of Chemistry and Environmental Science, Lanzhou City University, Lanzhou 730070, China.

*Corresponding authors. magf@nwnu.edu.cn (G. Ma), leizq@nwnu.edu.cn (Z. Lei).

‡ These authors contributed equally to this work.

Materials Characterizations

The morphology of the synthesized materials was examined using the FE-SEM (Ultra Plus, Carl Zeiss) and the same FE-SEM microscope was used to obtain energy dispersed X-ray spectroscopy (EDS). The structures of the synthesized materials were further carried out by TEM (FEI Tecnai G2 F20 S-Twin, USA). X-ray diffraction (XRD) data were taken from a D/Max-2400 (Rigaku) X-ray diffractometer with Cu K α radiation ($\lambda=1.5418\text{\AA}$). X-ray photoelectron spectra (XPS) were acquired on an Escalab 210 system (Germany) photoelectron spectrometer with an excitation source of Al K α radiation. The electrochemical properties of the fabricated devices were investigated by cyclic voltammetry (CV), galvanostatic charge/discharge (GCD), and electrochemical impedance spectroscopy (EIS) measurements using a CHI760E electrochemical workstation (Shanghai Chenchua instrument Co., Ltd., China). The cycle-life stability was performed using computer controlled cycling equipment (CT2001A, Wuhan Land Electronics Co., Ltd., China).

Electrochemical measurements

A typical three-electrode test cells in electrolyte was used for electrochemical measurement on CHI760D (Chenchua, Shanghai China) electrochemical working station. The Ni Foam supported CMOH and CMS was used as a working electrode. The mass of active material of the CMOH electrode on Ni foam was about 2.1 mg/cm², while the mass of active material of the CMS electrode Ni foam was about 2 mg/cm². An Hg/HgO reference electrode and carbon rod counter electrode were placed in 2 M KOH aqueous electrolyte.

On the basis of the following Equation 1, the area capacity (mAh cm⁻²) of battery-type materials was worked out from the charge-discharge graph:

$$C_A = I\Delta t/S \quad (1)$$

Similarly, the gravimetric capacity (mAh g⁻¹) of battery-type electrode materials was calculated from galvanostatic discharge by using the following formula:

$$C_g = I\Delta t/m \quad (2)$$

where, C_A is the area capacity (mAh cm⁻²), C_g is the gravimetric capacity (mAh g⁻¹), I is the current (A), Δt is the discharge time (s), S is the area of the electrode (cm²) and m is the mass of battery-type electrode materials.

The gravimetric specific capacitance (F g⁻¹) of carbon-based materials (electric double layer capacitor) was calculated from galvanostatic discharge by using the following formula:

$$C_s = I\Delta t/(m\Delta V) \quad (3)$$

An asymmetric supercapacitor device was assembled by using the CMS positive electrode, activated carbon negative electrode and a cellulose paper separator in a 2 M KOH electrolyte. The mass balancing will be exhibited in the following Eq. 4, so as to achieve $q^+ = q^-$ and take advantage of the largest voltage window. The specific capacitance (C_s), specific energy (E), and specific power (P) were calculated based on the total mass of the active materials using Eqs. 4–7.^[S1-S2]

$$m^+/m^- = C^+\Delta V/C^-\Delta V \quad (4)$$

$$C_s = I \cdot \Delta t / \Delta V \cdot m \quad (5)$$

$$E = \frac{1}{3.6m} \int_0^{V_{max}} I \cdot V dt \quad (6)$$

$$P = E / \Delta t \quad (7)$$

In Eqs. 5, the m is the total mass of the positive electrode and the negative electrode.

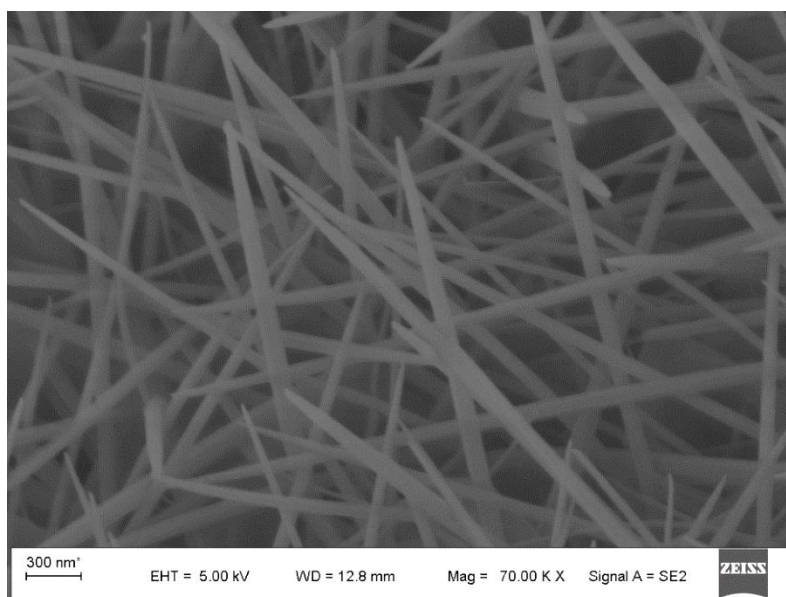


Fig. S1 SEM images of CMOH precursor at high magnification.

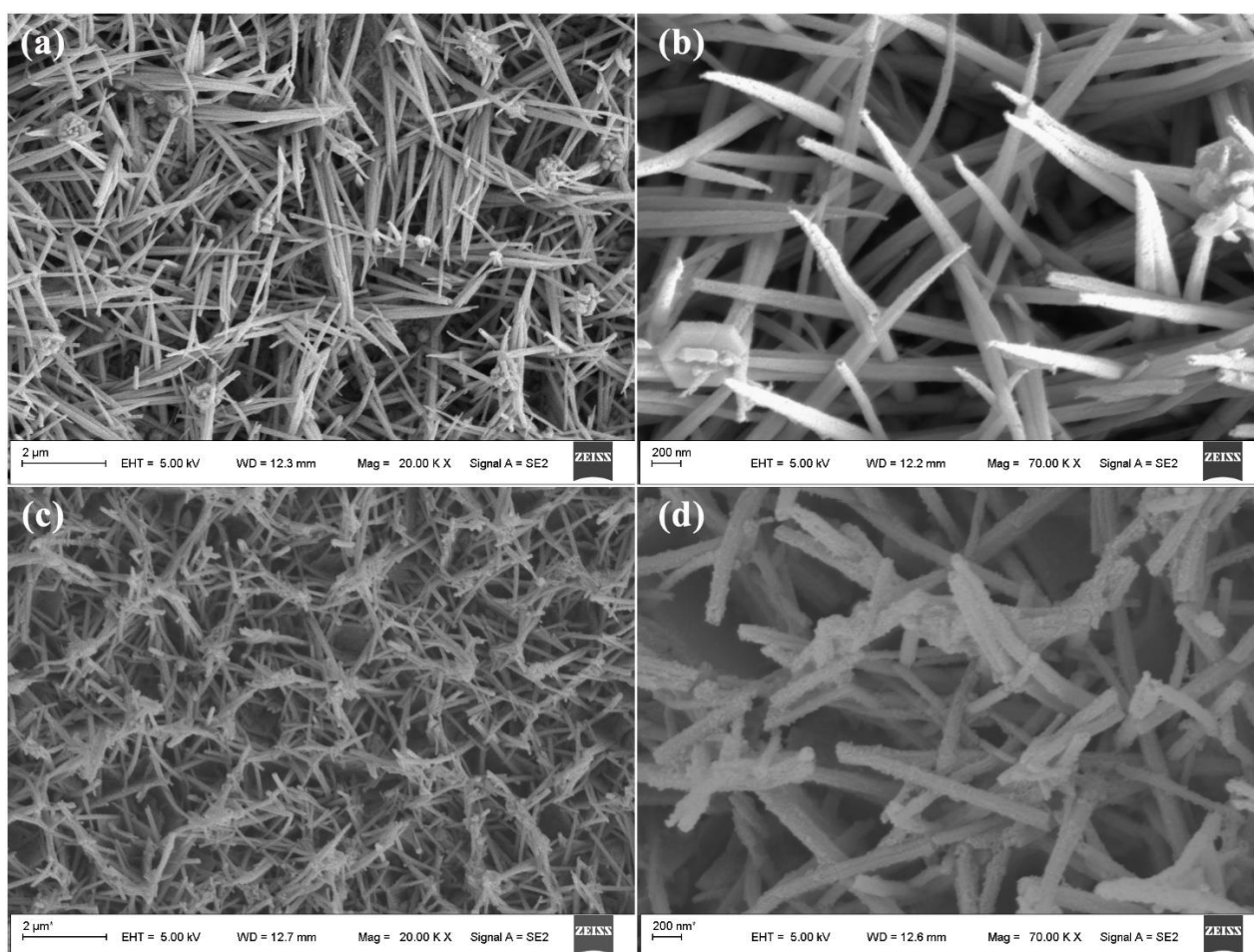


Fig. S2 SEM images of (a-b) CMS-6 and (c-d) CMS-10 nanoneedle arrays at different magnification.

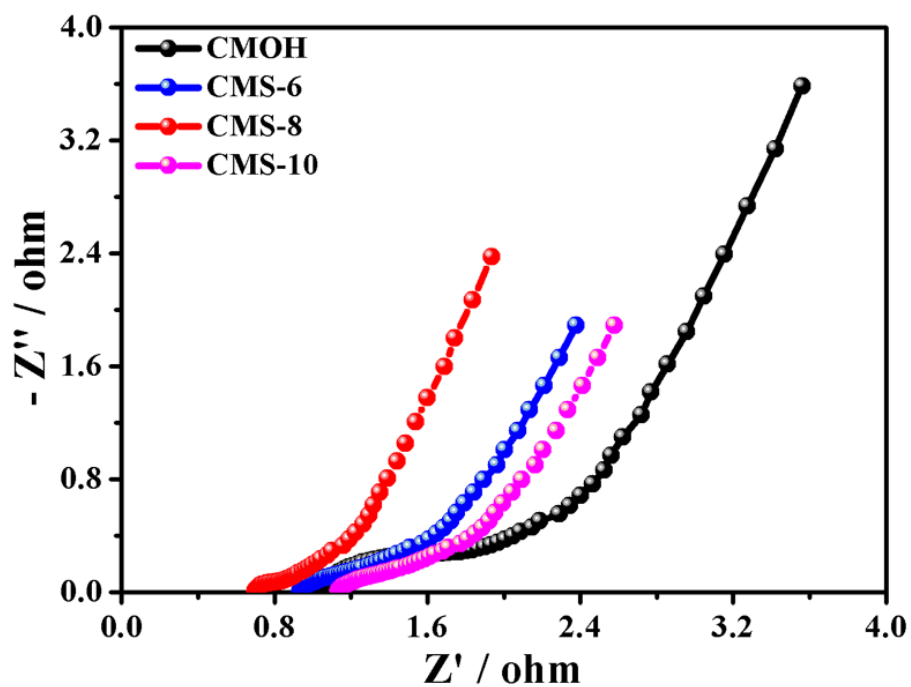


Fig. S3 EIS curves of the CMS nanoneedle arrays and CMOH precursor electrodes.

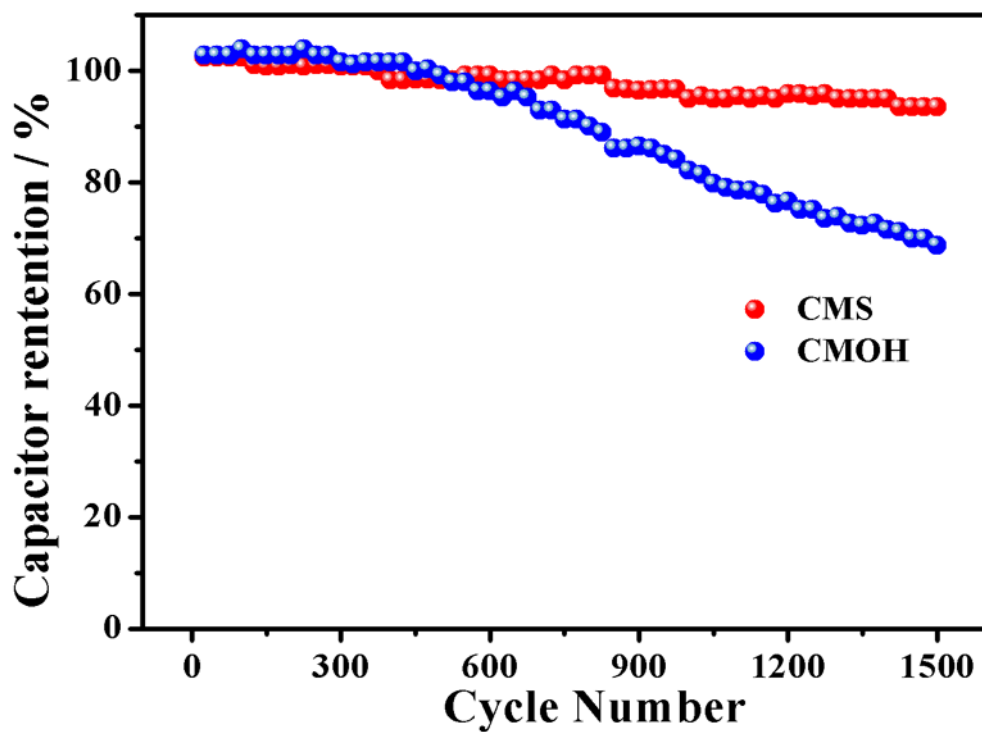


Fig. S4 Cyclic stability of the CMS-8 and CMOH electrodes over 1500 cycles at 5 A g^{-1} .

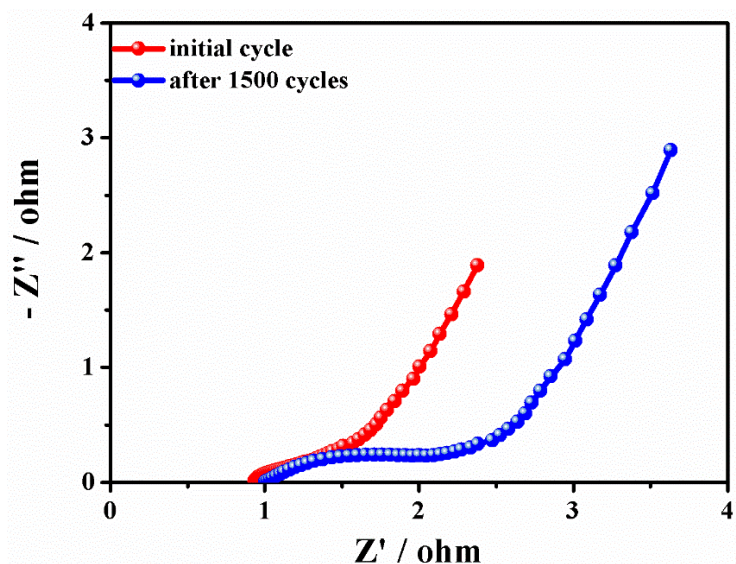


Fig. S5 Nyquist plots of the CMS-8 electrode before and after 1500 cycles.

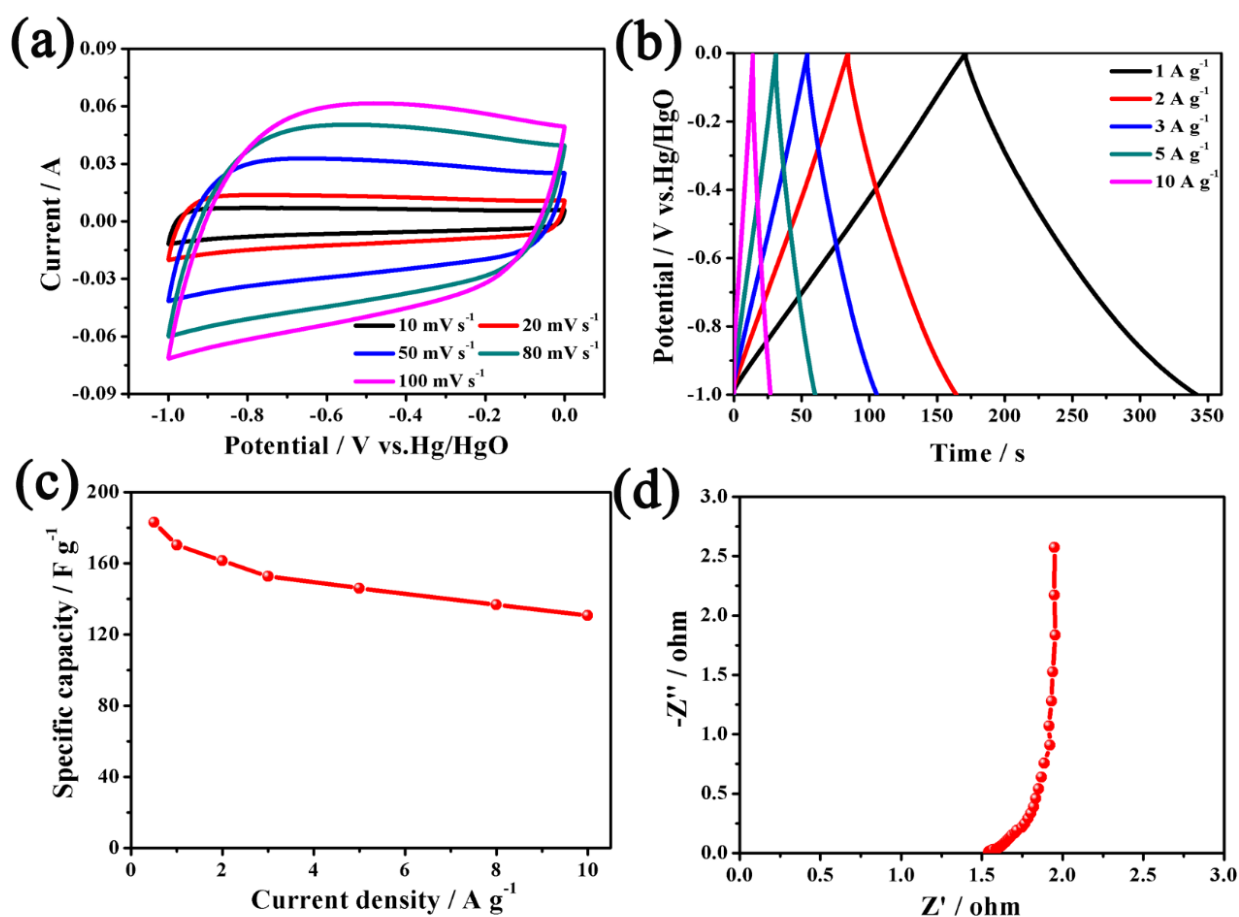


Fig. S6. (a) CV curves of AC at different scan rates. (b) GCD curves of AC at different current densities. (c) Specific capacitances of AC at different current densities. (d) EIS curve of the AC electrode

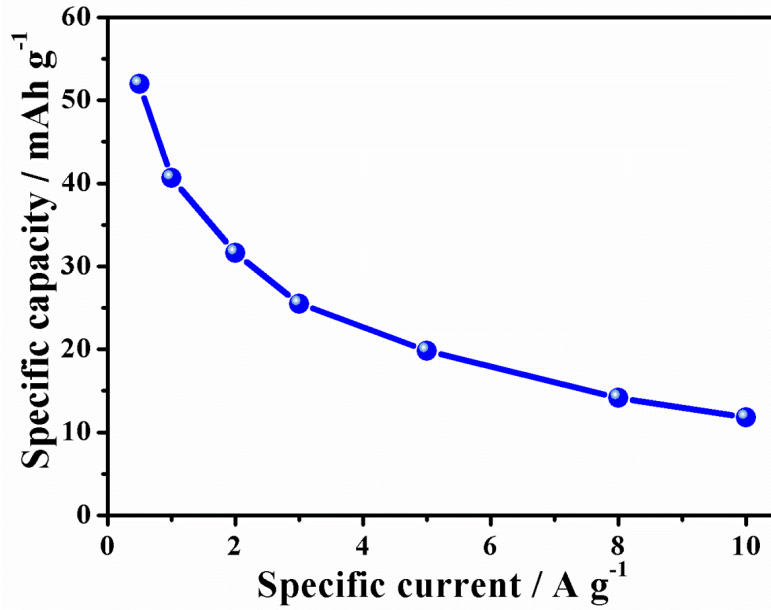


Fig. S7. Specific capacities of CMS-8//AC ASC device at different current densities.

Table S1. Comparison of the electrochemical performances of the CMS-8 electrode and those of some metal chalcogenides electrode materials.

Electrodes	Synthesis method	Electrolyte	Specific capacity (mAh g ⁻¹)	Test condition	Cyclic performance	Ref.
CMS-8	Hydrothermal	2 M KOH	351 (0.53 mAh cm ⁻²)	1 A g ⁻¹ (2 mA cm ⁻²)	93.7% (after 1500 cycles)	This work
Ni ₃ S ₂ nanoparticles	Hydrothermal	2 M KOH	110.3	2 A g ⁻¹	86.5% (after 1000 cycles)	[S3]
MoS ₂ @MPC	Mechanical exfoliation	1M H ₂ SO ₄	42	1 A g ⁻¹	96% (after 3000 cycles)	[S4]
NiSe@MoSe ₂	Hydrothermal	2 M KOH	128	1 A g ⁻¹	93.7% (after 1000 cycles)	[S5]
NiCo ₂ S ₄	Hydrothermal	2 M KOH	103	1 A g ⁻¹	93.4% (after 1500 cycles)	[S6]
Co _{0.85} Se	Hydrothermal	2 M KOH	50	0.5 A g ⁻¹	-	[S7]
NiSe ₂ hexapods	Hydrothermal	1M KOH	5.33	1 A g ⁻¹	~94% (after 5000 cycles)	[S8]
CuCo ₂ S ₄	Hydrothermal	2 M KOH	55.46	1 A g ⁻¹	83% (after 10000 cycles)	[S9]
NiS	Hydrothermal	2 M KOH	146	1 A g ⁻¹	90.2% (after 3000 cycles)	[S10]
Ni ₃ S ₂ /CNTs	Hydrothermal	2 M KOH	113.3	1 A g ⁻¹	80% (after 1000 cycles)	[S11]
NiS box-in-box	Hydrothermal	3 M KOH	92.8	1 A g ⁻¹	93.4% (after 3000 cycles)	[S12]

References

- (S1) X. Song, C. Huang, Y. Qin, H. Li, H. Chen, *J. Mater. Chem. A*, 2018, **6**, 16205-16212.
- (S2) G. Nagaraju, S. Cha, S. Sekhar, J. Yu, *Adv. Energy Mater.*, 2017, **7**, 1601362.
- (S3) W. Yu, W. Lin, X. Shao, Z. Hu, R. Li, D. Yuan, *J. Power Sources*, 2014, **272**, 137-143.
- (S4) Q. Weng, X. Wang, X. Wang, C. Zhang, X. Jiang, Y. Bando, et al., *J. Mater. Chem. A*, 2015, **3**, 3097.
- (S5) H. Peng, J. Zhou, K. Sun, G. Ma, Z. Zhang, E. Feng, et al., *ACS Sustain. Chem. Eng.*, 2017, **5**, 5951-5963.
- (S6) Z. Wu, X. Pu, X. Ji, Y. Zhu, M. Jing, Q. Chen, et al., *Electrochim. Acta*, 2015, **174**, 238-245.
- (S7) H. Peng, G. Ma, K. Sun, Z. Zhang, J. Li, Z. Zhou, et al., *J. Power Sources*, 2015, **297**, 351-358.
- (S8) N. S. Arul, J. I. Han, *Mater. Lett.*, 2016, **181**, 345-349.
- (S9) Y. Wang, D. Yang, T. Zhou, *Nanotechnology*, 2017, **28**, 465402.
- (S10) J. Yang, X. Duan, W. Guo, D. Li, H. Zhang, W. Zheng, *Nano Energy*, 2015, **5**, 74-81.
- (S11) C. Dai, P. Chien, J. Lin, S. Chou, W. Wu, P. Li, et al., *ACS. Appl. Mater. Interfaces.*, 2013, **5**, 12168-12174.
- (S12) X. Yu, L. Yu, L. Shen, X. Song, H. Chen, X. W. Lou, *Adv. Funct. Mater.*, 2014, **24**, 7440-7446.